Copper (I) Complexes of Zwitterionic Imidazolium-2-Amidinates, A Promising Class of Electroneutral, Amidinate-Type ligands

Astrid Márquez, Elena Ávila, Carmen Urbaneja, Eleuterio Álvarez, Pilar Palma and Juan Cámpora.*

Instituto de Investigaciones Químicas, CSIC – Universidad de Sevilla. C/ Américo Vespucio, 49, 41092, Sevilla, Spain.

ABSTRACT. The first complexes containing imidazolium-2-amidinates as ligands (betaine-type adducts of imidazolium-based carbenes and carbodiimides, NHC-CDI) are reported. Interaction of the sterically hindered betaines ICyCDI^{DiPP} and IMeCDI^{DiPP} (both bearing 2,6-diisopropylphenyl (DiPP) substituents on the terminal N atoms), with Cu(I) acetate affords mononuclear, electroneutral complexes **1a** and **1b**, which contain NHC-CDI and acetate ligands terminally bound to linear Cu(I) centers. In contrast, the less encumbered ligand ICyCDI$^{p\text{-Tol}}$, with p-tolyl substituents on the nitrogen donor atoms, affords a dicationic trigonal paddlewheel complex, $[Cu_2(\mu\text{-ICyCDI}^{p\text{-Tol}})_3]^{2+}[OAc^-]_2$ (**2-OAc**). The NMR resonances of this compound are broad and indicate that in solution the acetate anion and the betaine ligands compete for binding the Cu atom. Replacing the external acetate for the less coordinating tetraphenylborate anion provides the corresponding derivative **2-BPh$_4$** that, in contrast with **2-OAc**, gives rise to sharp

and well-defined NMR spectra. The short Cu-Cu distance in the binuclear dication $[Cu_2(\mu\text{-ICyCDI}^{p\text{-Tol}})_3]^{2+}$ observed in the X-ray structures of **2-BPh$_4$** and **2-OAc**, *ca*. 2.42 Å, points to a relatively strong "cuprophilic" interaction. Attempts to force the bridging coordination mode of $IMeCDI^{DiPP}$ displacing the acetate anion with BPh_4^- led to the isolation of the cationic mononuclear derivative $[Cu(IMeCDI^{DiPP})_2]^+[BPh_4]^-$ (**3b**) that contains two terminally bound betaine ligands. Compound **3b** readily decomposes on heating, cleanly affording the bis-carbene complex $[Cu(IMe)_2]^+[BPh_4^-]$ (**4**) and releasing the corresponding carbodiimide ($C(=N\text{-DiPP})_2$).

INTRODUCTION

Amidinates are an important class of ligands, characterized by the proximity of two potentially binding and electronically conjugated nitrogen atoms.[1] They can be seen as the nitrogen analogues of carboxylates, accordingly they share in common with these many aspects of their rich coordination chemistry. For example, carboxylates and amidinates usually coordinate in the monodentate (A), bidentate (B) or bridge (C) modes, shown in the upper part of Figure 1. In the bridging coordination mode, they give rise to a series of appealing multi-bridged binuclear "paddlewheel" complexes (D and E, Figure 1, down).[1,2] This type of compounds are also formed by related ligands bearing vicinal N donors, such as guanidinates.[1,3]

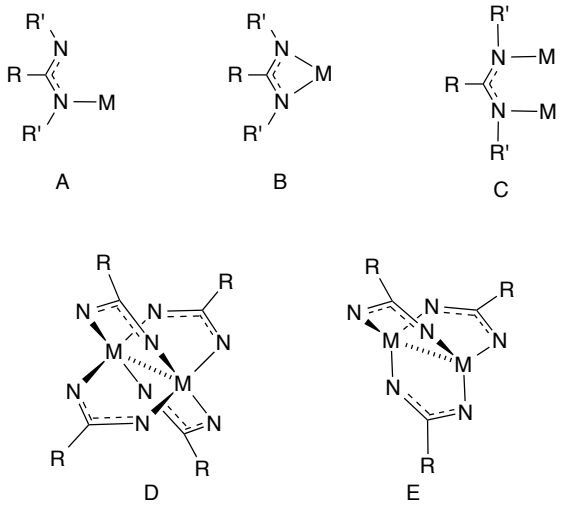

Figure 1. A – C, main coordination modes of amidinate (R = H, Alkyl or Aryl) or guanidinate (R = NR_2) ligands. D and E, tetragonal and trigonal paddlewheel complexes (R' omitted for clarity).

A significant difference between carboxylates and their nitrogen analogues is the presence of additional organic substituents (R') on the terminal N donor atoms of the latter, that allow for a more precise tuning of steric and electronic properties. This has prompted for the intensive application of amidinates and guanidinates in homogeneous catalysis, particularly in olefin polymerization,[4] and spurred the development of their coordination chemistry. The design of new catalyst architectures based on amidinate ligands has often been guided by analogies. Thus, when considering early transition or *f*-block elements, amidinates are regarded as "steric equivalents" of the ubiquitous cyclopentadienyl ligands.[1a,5] Although this concept loses usefulness on moving to catalysts based on late transition elements, whose design is often inspired by the highly successful Ni and Pd α-diimine complexes, analogy reasoning remains useful since both α-diimine and amidinate chelates[5,6] are built on trigonal sp^2 nitrogen centers that can be similarly substituted with bulky organic groups, such as 2,6-dialkylaryls. The main difference between the α-diimine and amidinate families of ligands is the electric charge, which

results in very different chemistries. In this context, we decided that the analogy between α-diimines and amidinates could be strengthened if the latter ligands could be modified somehow to render them electrically neutral. Seeking examples of neutral ligands bearing two sp^2 nitrogen donor centers adjacent to a single carbon atom, we realized that there exist very few molecules that fulfill such requirements. A rather unique example of such ligands would be 1,8-naphtyridines, naphthalene derivatives in which the vicinal CH groups in the positions 1 and 8 are replaced by N atoms. The coordination chemistry of these ligands has been extensively developed,[7] but lacking the possibility of attaching additional organic substituents to the nitrogen atoms, their coordination chemistry is peculiar and usually quite different of that of α-diimines.

In our search for new types of ligands that could match our concept of "neutral amidinates" we considered the possibility of building betaine-type zwitterions in which a positively charged fragment would counterbalance the negative charge of the amidinate donor group. While developing this idea, we came across betaine adducts of heterocyclic carbenes (NHC) with carbodiimides (CDI).[8] By analogy with the well-known NHC-CO_2 adducts, or imidazolium-2-carboxylates,[9] NHC-CDI adducts could be termed "imidazolium-2-amidinates" (Figure 2). The first example of such a compound was $Me_2IMeCDI^{iPr}$, prepared in 1999 by Kuhn and co-workers by addition of the imidazole-based carbene 1,2,3,4-tetramethylimidazol-2-ylidene (Me_2IMe) to diisopropylcarbodiimide (CDI^{iPr}).[10] They reported the crystal structure and some chemical properties of this compound, which confirm that this has a true dipolar structure. As such, it exhibits a strong Brönsted basicity on the terminal "amidinate" nitrogen atoms. Very recently, Johnson and co-workers reported that similar betaines, $SIArCDI^{Ar}$, are spontaneously formed in the thermal decomposition of 2,3-diarylimidazolidin-2-ylidenes (SIAr). They also prepared a series of new NHC-CDI adducts starting from carbodiimides by Kuhn's method.[11]

Simultaneously, we showed that the adduct ICyCDI^{pTol} acts as a stabilizing ligand for Ru nanoparticles, allowing control over their size and selectivity in styrene hydrogenation.[12] We believe that these betaines bind adjacent metal centers on the surface of the nanoparticles (coordination type C in Figure 1). Furthermore, we expected that, analogously to amidinate ligands, NHC-CDI betaines could also coordinate in the terminal (A) or bidentate (B) modes, and that their binding preferences could be controlled through the steric and electronic properties of their substituents. Surprisingly enough, no complexes of carbene-carbodiimide betaines with either transition or main group metals appear to have been ever described so far. As a preliminary step before pursuing the development of transition metal-based catalysts for olefin polymerization based on NHC-CDI adducts, or other catalytic reactions, we decided to explore their coordination to a diamagnetic Cu(I) center. Herein we report the results of this study.

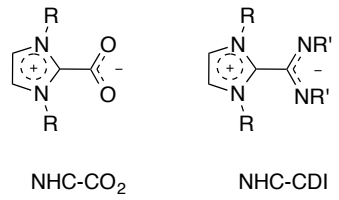

Figure 2. Imidazolium-2-carboxylate (NHC-CO_2, left) and imidazolium-2-amidinate (NHC-CDI, right).

RESULTS AND DISCUSSION

As shown in Scheme 1, the present work focuses on three NHC-CDI adducts that are combinations of imidazolium-based heterocyclic carbenes (NHC's) containing either cyclohexyl (ICy) or methyl (IMe) substituents at the nitrogen atoms, with di-*p*-tolyl or di-2,6-diisopropylphenylcarbodiimide (CDI^{pTol} or CDI^{DiPP}, respectively). The heterocyclic carbenes were generated in THF solution by deprotonation of the corresponding imidazolium salts with

KO*t*Bu and then reacted *in situ* with the suitable carbodiimide. It must be mentioned that, in contrast with the thermally robust ICy carbene, IMe is relatively unstable and, in order to obtain satisfactory results, its solution should not be allowed to warm to the room temperature, until it is reacted with the carbodiimide. The corresponding NHC-CDI adducts were easily isolated in high yields as yellow solids, stable in the open atmosphere (although in the long term they are best stored under nitrogen), very soluble in CH_2Cl_2 and only slightly in toluene or hydrocarbon solvents. Surprisingly, their solubility in THF is only moderate. The yellow color of these compounds is due to the lowest frequency absorption of a series of overlapping intense UV bands, which occurs at *ca*. 350 nm and tails into the visible zone. The fact that the alkyl-substituted betaine adduct Me_2IMeCDI^{iPr} reported by Kuhn is colorless,[10] indicates that the color-responsible transition involves the π orbitals of the aryl rings bound to the amidinate N atoms. A TD-DFT calculation (see SI) shows that the lowest energy band corresponds to an electronic transition from the HOMO, a π-orbital centered mainly on the anionic amidinate group, to the LUMO, which pertains mainly to the cationic heterocyclic fragment. The energy of this transition is lowered because the HOMO is destabilized by a non-bonding interaction with filled π orbitals of the aryl substituents. The color-responsible absorption is most intense in the bright yellow derivative ICyCDI^{pTol}, but neither this nor ICyCDI^{DiPP} or IMeCDI^{DiPP} exhibit fluorescence, as reported by Johnson for betaines carrying aryl substituents in all four nitrogen atoms.[11] The IR spectra of our three betaines display a medium intensity band at ca. 1600 cm^{-1} and a complex superposition of intense bands in the 1550 -1510 cm^{-1} region. DFT analysis of a simplified molecular model suggests that the former absorption corresponds to the asymmetric NCN stretch of the terminal "amidinate" fragment, and the latter arise from a combination of C=N stretchs (either from the amidinate and the imidazolium units) and C-H flexion modes.

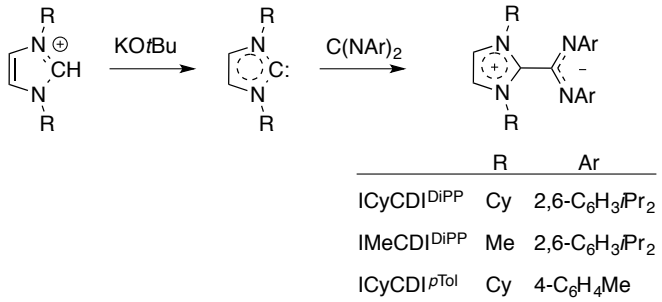

	R	Ar
ICyCDI^{DiPP}	Cy	2,6-C_6H_3*i*Pr_2
IMeCDI^{DiPP}	Me	2,6-C_6H_3*i*Pr_2
ICyCDI^{pTol}	Cy	4-C_6H_4Me

Scheme 1.

The solution NMR spectra of the betaines are relatively simple, for both imidazolium (R) or amidinate (Ar) substituent groups are chemically equivalent, each of them giving rise to single set of signals. For ICyCDI^{DiPP}, the signals of the diastereotopic Me groups of the DiPP unit (DiPP = 2,6-diisopropylphenyl) are well resolved in the ^{1}H and $^{13}C\{^{1}H\}$ NMR spectra at room temperature. In contrast, the DiPP methyls of the less bulky derivative IMeCDI^{DiPP} give rise to a single resonance in the ^{1}H spectrum, and to two broad ^{13}C NMR resonances. This indicates that for ICyCDI^{DiPP}, rotation of the DiPP groups is locked in the NMR timescale, whereas they undergo restricted rotation for IMeCDI^{DiPP}. Due to the symmetrical substitution pattern of the CDI-NHC adducts, their NMR spectra provide no indication as to whether the imidazolyl ring and amidinate moieties rotate one with regard to the other, therefore they give no direct evidence on the existence or not of some π delocalization over the central C-C bond that connects them. Charge separation has seemingly little influence in the position of the ^{13}C NMR resonances of the corresponding quaternary carbon atoms of the imidazole ring and the amidinate fragment, as they appear in very close positions, between 145 and 150 ppm.

The crystal structure of the three NHC-CDI adducts have been determined. As they are very similar, only the ORTEP view of ICyCDI^{DiPP} with indication of key atoms is shown in Figure 3. Plots of IMeCDI^{DiPP} and ICyCDI$^{p\text{-}Tol}$ can be found in the SI (Figures S2 and S3), and

selected bond distances and angles for the three compounds are collected in Table 1. The three structures show identical conformations. The C-N bonds of the amidinate moiety adopt different configurations, one cisoid and the other transoid with regard to the imidazolyl and aryl groups. This is the same observed by Kuhn for $Me_2IMeCDI^{iPr}$,[10] but different from that of Johnson's betaines (recall that these bear bulky aryl rings both in the heterocycle and the amidinate N atoms), in which both nitrogen substituents are *trans* with regard the imidazole ring.[11] As mentioned before, solution NMR spectra show single set of signals for the aryl substituents of the amidinate fragment, but in the solid state, the preferred cis-trans configuration of the amidine renders the aryl substituents chemically non-equivalent. This indicates that the geometry of the C-N bonds is labile and they rapidly exchange their configuration in solution.

The main metric parameters in the three compounds are almost identical to those of the previously reported NHC-CDI betaines.[10,11] Independently of their configuration, the amidinate C-N bond lengths are within a narrow range, 1.31 - 1.33 Å, and those of the imidazolyl fragments are only slightly longer, 1.34 – 1.35 Å. These distances can be regarded as typical for delocalized, partially double bonds. Conversely, the C-C bonds between both moieties, close to 1.505 Å, are consistent with pure σ character. The imidazolium rings are always rotated by nearly 60º with regard to the corresponding amidinate fragment. Curiously, the amidinate N_t-C-N_c angles are somewhat narrower in $ICyCDI^{DiPP}$ (126.5º) and $IMeCDI^{DiPP}$ (127.5º) than in $IMeCDI^{pTol}$ (130.1º), in spite of the considerable steric bulk of the DiPP substituent.

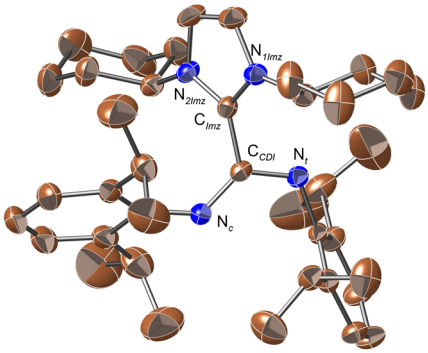

Figure 3. ORTEP view (50 % probability ellipsoids) of ICyCDI^{DiPP}

Table 1. Selected bond distances (Å) and angles (deg) for NHC-CDI adducts.[a]

	ICy-CDI^{DiPP}	IMe-CDI^{DiPP}	ICy-CDI^{pTol}
		Distances	
C_{CDI}-N_C	1.315(3)	1.312(5)	1.3302(16)
C_{CDI}-N_t	1.313(3)	1.319(5)	1.3202(16)
C_{CDI}-C_{imz}	1.502(3)	1.505(6)	1.5044(18)
C_{imz}-N_{1imz}	1.349(3)	1.347(5)	1.3415(16)
C_{imz}-N_{2im}	1.339(4)	1.340(5)	1.3448(17)
		Angles	
N_t-C_{CDI}-N_c	126.5(2)	127.5(4)	130.12(12)
N_{1imz}-C_{imz}-N_{2imz}	107.5(2)	106.7(4)	107.52(11)
CDI∠imz[b]	54.6	50.2	54.9

a) For ORTEP views and full numbering schemes, see SI. *b*) Torsion angles between the mean planes defined by atoms N_c, N_t, C_{CDI}, C_{imz} and N_{1imz}, N_{2imz}, C_{imz}, C_{CDI}.

To investigate the coordination chemistry of the NHC-CDI adducts, we chose to study their interaction with Cu(I) acetate. In addition to the known ability of Cu(I) to bind many different types of ligands and its diamagnetic character, we selected this starting material because

the potentially bridging acetate ligand might be complementary to the electroneutral NHC-CDI unit, giving rise to multinuclear assemblies simultaneously bridged by both ligands, as observed in a number of acetate-amidinate complexes.[13] Copper(I) acetate forms itself a infinite planar chains composed of $Cu_2(\mu\text{-}OAc)_2$ dimers enchained through secondary bridging Cu···O interactions.[14] However, we never observed simultaneous acetate/betaine coordination in our complexes. Scheme 2 summarizes the reactivity of Cu(I) acetate with these betaine-type ligands. The different products were fully characterized by NMR (^1H, ^{13}C and a range of binuclear homo- and heterocorrelation spectra) IR, UV-VIS and elemental analysis, and their X-ray structures were determined in all cases.

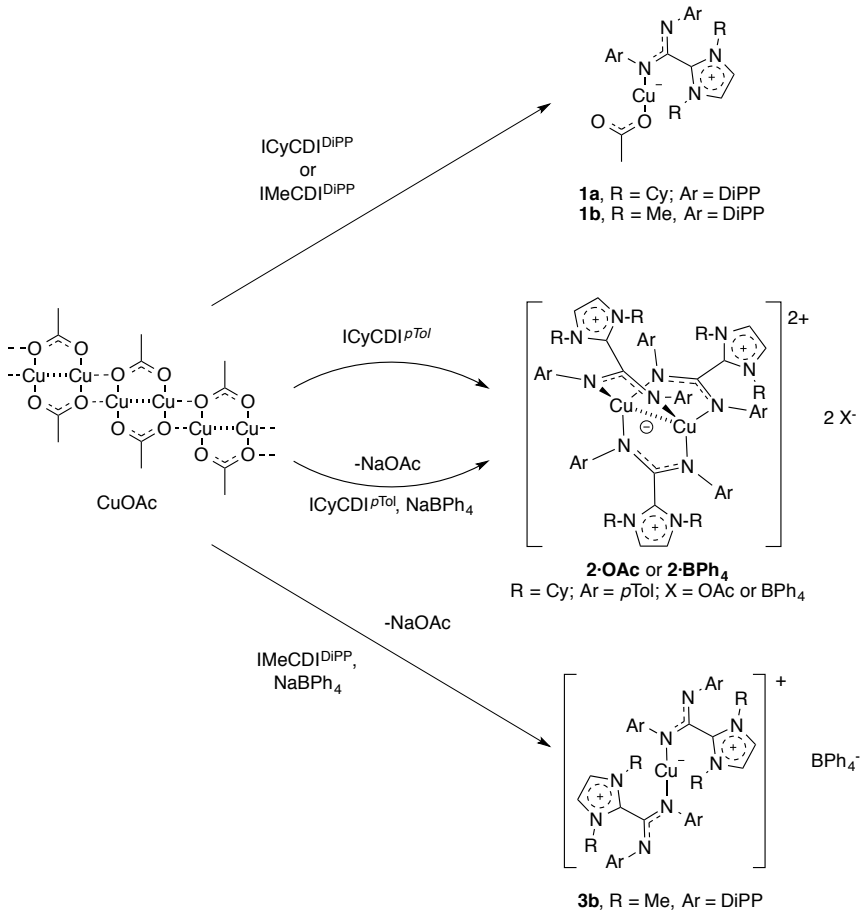

Scheme 2.

The interaction of Cu(I) acetate with equimolar amounts of ICyCDI^{DiPP} or IMeCDI^{DiPP} leads to the formation of pale yellow-green 1:1 (CuOAc)(L) complexes, **1a** and **1b**, respectively. Their crystal structures are shown in Figure 4, and selected bond lengths and angles are listed in Table 2. Both structures show a single Cu atom with terminally coordinated NHC-CDI and acetate ligands in a linear arrangement. In these compounds, the betaine ligands have the same configuration observed in the crystal structures of the free ligands. The copper atom coordinates the amidinate nitrogen atom of the "transoid" C=N bond (N_t), leaving free the one in the "cisoid"-configured bond (N_c). The mean planes defined by the imidazole and the amidinate groups are rotated by similar amounts in the complexes and in the free ligands, ca. 60º. The coordinated trans C-N amidinate bond is significantly longer (ca. 1.35 Å) than the free cis C-N bond (ca. 1.29 Å). A similar difference is noted between the coordinated and free C-O bonds of the monohapto acetate ligand. This effect can be attributed to the localization of the π bonding upon coordination to the metal center.

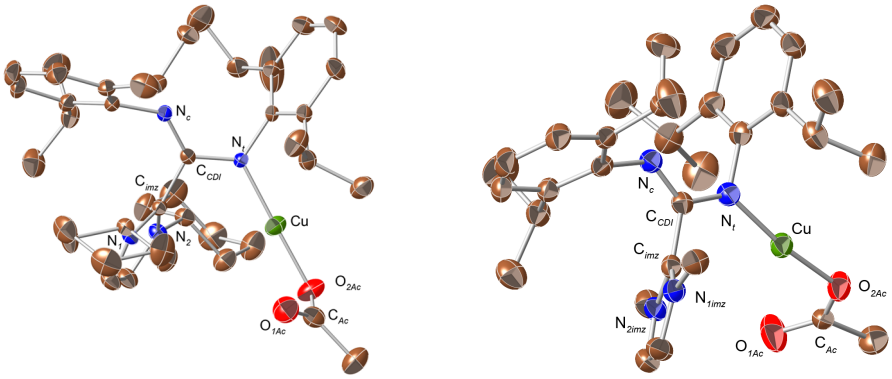

Figure 4. ORTEP view (50 % probability ellipsoids) of compounds **1a** (left) and **1b** (right). For a list of selected bond distances and angles see Table 2.

The NMR signals of the betaine ligands are easily recognized and have been precisely assigned with the aid of full range of 2D homo- (COSY, NOESY) and heterocorrelation (HSQC, HMBC) spectra. In contrast, those of the acetate are very broad and hardly identifiable (in special in the $^{13}C\{^{1}H\}$ spectrum), presumably because in both **1a** and **1b** this ligand undergoes intermolecular exchange. The room temperature NMR spectra of **1a** and **1b** in CD_2Cl_2 suggest that the monodentate coordination of the amidinate ligands is maintained in solution, at least in non-coordinating solvents (the ^{1}H spectrum of **1a** is shown in the SI, see Figure S7). This is readily deduced from the fact that they display single sets of signals for the imidazolium H and R substituents (R = Cy and Me in **1a** and **1b**, respectively), but two sets of signals for the aryl substituents of the amidinate, indicating that these become non-equivalent. For both **1a** and **1b**, the signals of one of the DiPP groups appear perfectly sharp, but those of the other are very broad, particularly in the ^{1}H spectra which shows the diastereotopic iPr methyl signals close to the coalescence (**1a**) or already forming a single broad hump (**1b**). This selective line broadening indicates that the DiPP group responsible for the broad signals is undergoing restricted rotation on the NMR timescale, whereas the other is fixed in its position, presumably due to the steric bulk of the coordinated Cu(OAc) fragment. Monodimensional spectra provide no evidences of any further dynamic effects, but phase-sensitive 2D NOESY/EXSY for both **1a** and **1b** clearly shows exchange cross-peaks linking the signals of the two types of DiPP groups, implying that the Cu(OAc) fragment is actually jumping from one amidinate nitrogen atom to the other. In the case of **1a** this movement must involve simultaneous cis/trans isomerization of the C-N bonds because the exchange of the Cu atom does not lead to the appearance of any isomeric forms of the complex. However, both the ^{1}H and the $^{13}C\{^{1}H\}$ spectra of **1b** show the presence of a minor species that is invariably in *ca.* 1:6 intensity ratio with regard to the main complex. This is

presumably a geometric isomer resulting from the migration of the Cu atom to the nitrogen atom of the cisoid C-N bond. The observation of two independent DiPP sets also in this minor isomer is consistent with this assignment, as it indicates that the increased steric crowding hinders the rotation of not just one but both DiPP rings.

In contrast with the well-defined and informative NMR spectra of compounds **1a** and **1b**, those of the orange product **2·OAc**, isolated from the reaction of CuOAc with ICyCDI$^{p\text{-Tol}}$, show very broad lines at the room temperature. However, the ^{1}H spectrum shows two readily recognizable signals in 3:1 intensity ratio, one at δ 2.23 ppm for the tolyl *p*-Me group and the other at δ 4.39 ppm for the 1-CH of the Cy groups, which suggest a symmetrical structure. The X-ray structure of this compound (see SI, Figure S4) reveals a trigonal paddlewheel Cu complex, [Cu_2(ICyCDI^{pTol})$_3$] containing two Cu atoms bridged by betaine ligands, and free-standing acetate anions. Only one acetate per Cu_2 unit could be located in the electron density map, although on the basis of its diamagnetic character and its elemental analysis, the formula of **2·OAc** must be [Cu_2(μ-ICyCDI^{pTol})$_3$]$^{2+}$[AcO^-]$_2$. Likely, a disorder problem prevented the location of the missing acetate anion. Accordingly, the same compound was obtained when the reaction of ICyCDI$^{p\text{-Tol}}$ and CuOAc was carried in the correct 3:2 stoichiometric ratio. Complex **2-OAc** appears to be the only species formed in this system, regardless of whether reagent ratio was 3:2 or 1:1. The spontaneous assembly of this binuclear structure provides some support to our previous suggestion that ICyCDI$^{p\text{-Tol}}$ stabilizes small Ru nanoparticles by bridging adjacent metal atoms on their surface.[12]

In order to definitively clarify the identity of **2-OAc**, we decided to exchange the acetate anions with $NaBPh_4$. Thus, mixing ICyCDI$^{p\text{-Tol}}$, CuOAc and $NaBPh_4$ in 3:2:2 ratio in CH_2Cl_2

containing a small amount of THF to improve the solubility of the reagents, afforded the corresponding ionic complex **2·BPh$_4$**, which was isolated as brick-red crystals in excellent yield. The presence of the $[Cu_2(\mu\text{-ICyCDI}^{p\text{-Tol}})_3]^{2+}$ dication was confirmed by ESI-MS. When the spectrum of **2·BPh$_4$** was recorded from a CH_2Cl_2 solution, the main species observed in the gas phase was a monocation of composition $[Cu(ICyCDI^{p\text{-Tol}})_2]^+$ (m/z = 971.6), however a weak signal for the dication $[Cu_2(\mu\text{-ICyCDI}^{p\text{-Tol}})_3]^{2+}$ was also observed at the expected m/z of 744 with the correct isotope distribution and a spacing of half mass units between consecutive isotope peaks. The dication is probably destabilized in the gas phase due to the intramolecular coulombic repulsions, but optimum conditions for its observation were developed using different solvents. Best conditions for the observation of this signal were found using relatively non-coordinating dichloromethane or anisole as solvents.

Two types of crystals of **2·BPh$_4$** were grown using different methods. Cooling a saturated solution in a dichloromethane-toluene mixture in the freezer (-20 ºC) afforded solvent-free crystals, whereas layering a dichloromethane solution with toluene at room temperature produced a mixed solvate containing three molecules of toluene and five of dichloromethane per unit cell. The structural data from both structures are fully consistent (for details see Figure S5 and Table S2 in the SI) but the latter produced a slightly better quality X-ray structure, therefore the discussion will be referred to this dataset. An ORTEP view of the binuclear dication in **2·BPh$_4$** is shown in Figure 5. This is essentially the same found in **2·OAc**, with minimal differences of no chemical significance. As mentioned before, three betaine units act as bridging ligands between both Cu centers. The lengths of Cu-N bonds ligand termed “C” are nominally longer than those of ligands “A” and “B”. The difference, although statistically significant, is

very minor and is not observed in the solvent-free structure of **2·BPh$_4$**, nor in the cationic fragment of **2·OAc**, therefore it can be safely neglected. However the length of Cu-N bonds in

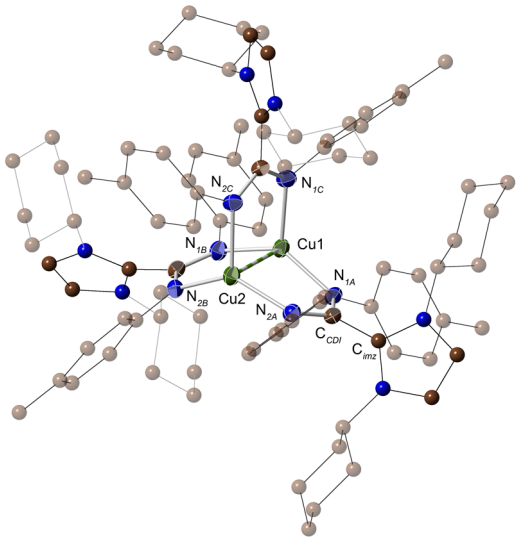

Figure 5. ORTEP view (50 % probability ellipsoids) of the cationic fragment of **2·BPh$_4$**. For clarity, only the atoms located in the Cu_2N_6 are represented as ellipsoids, and those in the Cy and *p*-tolyl groups are dimmed. Selected bond distances (Å) and angles (º): Cu1-Cu2, 2.4213(4); Cu1-N_{1A}, 1.965(2); Cu1-N_{1B}, 1.975(2); Cu1-N_{1C}, 2.066(2); Cu2-N_{2A}, 1.976(2); Cu2-N_{2B}, 1.970(2); Cu2-N_{2C}, 2.070(2); C_{CDI}-C_{imz} (ave.), 1.505(2); N_{1A}-Cu1-N_{1B}, 115.17(9); N_{1B}-Cu1-N_{1C}, 108.38(9); N_{1c}-Cu1-N_{1A}, 136.10(10); N_{1A}-Cu1-Cu2-N_{2A}, 9.53(9); N_{1B}-Cu1-Cu2-N_{2B}, 5.91(9); N_{1B}-Cu1-Cu2-N_{2B}, 10.16(9); Angle between imidazolyl and amidinate mean planes (ave.), 58.15.

the binuclear dication (average 2.00 Å in **2·BPh$_4$**) are significantly longer than those in complexes with monodentate betaine ligands (**1a**, 1.869; **1b**, 1.850 Å). Both CuN_3 units are very nearly flat, each Cu atom coming outside of plane defined by the three nitrogen atoms by only 0.07 Å. The average dihedral angles formed by each bridging betaine ligand and the copper atoms is small (average N-Cu-Cu-N = 8.5 º), therefore the CuN_3 units are close to an eclipsed

configuration. The Cu···Cu distance, 2.4213(4) Å, is rather short and clearly points to a closed shell (d^{10}-d^{10}) or "cuprophilic" interaction.[15] Interestingly, this distance is shorter than those in related $[Cu_2(\mu\text{-}L_n)]^{2+}$ complexes bridged by comparable electroneutral ligands such as the closely related N_2-donor 1,8-naphtyridyne (2.534 Å)[16] or bridging diphosphinomethanes (~2.73 Å),[15c,17] and ranges among the shortest Cu-Cu interactions observed in binuclear Cu(I) complexes bridged by anionic amidinate or guanidinate anions (2.40 – 2.54 Å).[18] This observation suggests that, although electrically neutral, the electronic influence of the betaine on the Cu atoms is more similar to that of related anionic ligands.

Although the solid-state structures of **2·OAc** and **2·BPh$_4$** contain the same $[Cu_2(ICyCDI^{p\text{-}Tol})_3]^{2+}$ subunit, their NMR spectra look very different, suggesting that the counterion has a deep effect on their solution behavior. Figure 6 shows a comparison of the ^{1}H NMR spectra of both compounds with that of the free ICyCDI$^{p\text{-}Tol}$ ligand. As can be seen, the sharp and well-defined signals in the spectrum of **2·BPh$_4$** contrast with the broad spectrum of **2·OAc**. In agreement with the high symmetry of the dicationic unit, both complexes give rise to a single set of signals for the betaine ligand, but their positions are quite different. For example, the resonance of the cyclohexyl 1-methyne signal (marked B in Figure 6) in **2·OAc** is 4.39 ppm, which is definitely closer to that of the free ligand (4.57 ppm) than to the analogous resonance in **2·BPh$_4$**, 3.59 ppm. In general, the signals of **2·BPh$_4$** exhibit stronger shifts relative to those of the free ligand than those of **2·OAc**. Noteworthy, the chemical shifts of the cyclohexyl or the imidazolium signals in the spectrum of **2·OAc** resemble more those observed in the spectrum of mononuclear **1a** (see Figure S7 in the SI), in which the ICyCDI^{DiPP} ligand coordinates in terminal mode, than to those of **2·BPh$_4$**. This suggests that the broad appearance of the NMR spectra of **2·OAc** could be due to the dynamic shift of the betaine ligand between the bridging and the

terminal coordination modes, presumably caused by the competition with the acetate anion for binding the Cu(I) center. Acetate does not displace the betaine fully, as the signals of the free ligand are not observed in the NMR spectra of **2·OAc**,

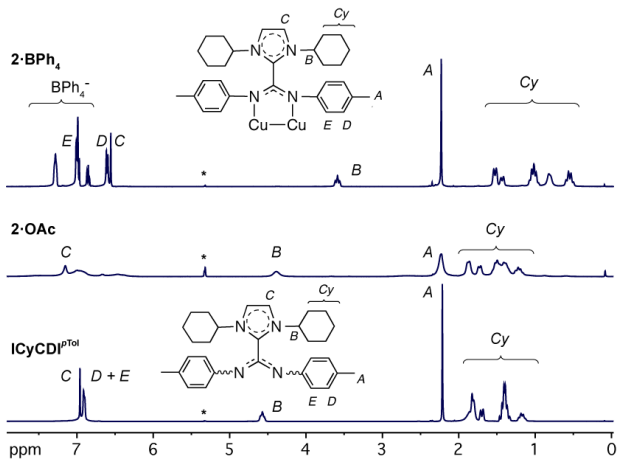

Figure 6 ^{1}H NMR spectra (CD_2Cl_2, 400 MHz, 298 K) of complexes **2·BPh$_4$**, **2·OAc** and the ligand ICy·CDI$^{p\text{Tol}}$. The solvent residual peak is marked with an asterisk.

neither at the room temperature nor below it. A VT-NMR ^{1}H study of **2·OAc** carried out between room temperature and -80 ºC showed that this compound exists in solution as a mixture of species, but static spectra were not observed even at the lowest temperature. Below -10 ºC, the spectrum resolves partially, showing at least three sets of signals, each of them showing a characteristic cyclohexyl methyne resonance. One of these Cy 1-C*H* signals appears at δ 3.61, hence it probably corresponds to the $[Cu_2(\mu\text{-ICyCDI}^{p\text{-Tol}})_3]^{2+}$ dication, whilst the higher field shifts of the other (δ 4.15 and 4.36 ppm, respectively) suggest that they arise from terminally-bound betaine ligands. The presence of betaine-bridged species in the solutions of **2·OAc** is also supported by their distinctive reddish-orange color, similar to that of the solid material or to **2·BPh$_4$** (either in solution or in the solid state) but contrasts with the very pale mononuclear

complexes **1a** and **1b**. The color of **2·OAc** or **2·BPh$_4$** is probably due to the presence of Cu···Cu interactions. For example, complexes [Cu$_2$(μ-dcpm)$_2$]X$_2$ give rise to absorption bands at 307 – 311 nm that have been assigned to metal-metal 3d→4p transitions.[15c] The UV-Vis spectra of both types of Cu(I) complexes, **1** and **2**, are monotonous curves with λ_{max} < 200 nm tailing into the visible region, doubtless due to the overlapping of a number of individual bands, as previously mentioned for the free ligands. However, the extinction in the visible region below 400 nm is considerably higher for **2·OAc** and **2·BPh$_4$**, the spectrum of the latter showing two shoulders whose frequencies (ca. 310 nm, ε ≈ 6000, and 370 nm, ε ≈ 3000 mol^{-1} l cm^{-1}) are similar to those in the aforementioned diphosphine-bridged complexes.

Next, we carried out the reaction of IMeCDI^{DiPP} with CuOAc in the presence NaBPh$_4$, reasoning that the removal of the acetate ligand would enable the bulky betaine to act as a bridge, giving rise to a binuclear product analogous to **2·BPh$_4$**. When we carried out the reaction in either 1:1:1 or 2:3:2 CuOAc/ligand/NaBPh$_4$ ratio, yellow-orange materials were obtained whose NMR spectra indicated the formation of a mixture containing two main species. However, upon recrystallization from a CH$_2$Cl$_2$/hexane mixture, pale yellow crystals containing a single product, **3b**, were obtained. The X-ray diffraction structure of this compound, shown in Figure 7 shows a mononuclear CuL$_2^+$ cation with two terminally bound betaine ligands. Main bond lengths and angles for this compound are collected in Table 2, where they can be compared with those of **1a** and **1b**. Although not affected by the crystal symmetry, each molecule has an effective center of symmetry in the Cu atom, therefore the configuration and metric parameters of both ligands are virtually the same. These are almost coplanar (the dihedral angle formed by the symmetrical $C_{CDI}(N_c)(N_l)(C_{imz})$ units is 24.8º). In spite of the cationic character of **3b**, its Cu-N bond distances

are nearly identical to those of the neutral **1b** (1.855 and 1.850 Å, respectively). Other internal measurements are also very nearly the same in both compounds.

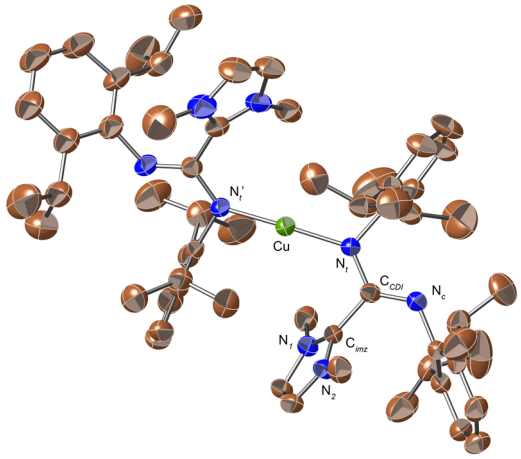

Figure 6. ORTEP view (50 % probability ellipsoids) of compound **3b**. For selected bond distances and angles, see Table 2.

Table 2. Selected bond distances (Å) and angles (deg) for compounds **1a**, **1b** and **3b**.

	1a	**1b**	**3b**
		Distances	
Cu-N_t	1.870(2)	1.8498(11)	1.855(2)
Cu-O_{2Ac}	1.843(2)	1.8460(11)	
C_{CDI}-N_c [a]	1.286(3)	1.2596(17)	1.292(4)
C_{CDI}-N_t	1.354(3)	1.3390(16)	1.348(4)
C_{CDI}-C_{imz}	1.503(3)	1.4493(18)	1.503(4)
C_{imz}-N_{1imz}	1.347(3)	1.3363(19)	1.334(4)
C_{imz}-N_{2im}	1.344(3)	1.3470(16)	1.340(4)
O_{2Ac}-C_{Ac}	1.277(4)	1.2555(17)	
O_{1Ac}-C_{Ac}	1.228(4)	1.2077(18)	

	Angles		
N_t-Cu-(O or N_t')	178.97(10)	171.24(5)	175.67(11)
N_c-C_{CDI}-N_t	122.9(2)	123.11(12)	123.1(3)
N_{1imz}-C_{imz}--N_{2imz}	107.3(2)	107.16(11)	107.1(3)
	Angles between planes[b]		
CDI∠imz	61.2	63.9	60.6
CDI∠L (L = OAc or CDI')	71.4	61.3	24.8

a) Averaged values from both $IMeCDI^{DiPP}$ ligands. *b)* Angle between mean planes containing amidinate CCN_2 or acetate CCO_2 atoms (CDI or OAc, respectively), or imidazolium ring (imz).

The room temperature NMR spectra of complex **3b** are well-defined and informative. They indicate that at both $IMeCDI^{DiPP}$ ligands are chemically equivalent, but they originate independent sets of signals for the coordinated and non-coordinated N-DiPP groups. Different from **1a** or **1b**, the room temperature NMR spectra of **3b** are purely static and show no signs of rotation of the DiPP groups, each of them giving rise to a pair of doublets for the diastereotopic *i*Pr methyls. The phase-sensitive ^{1}H NOESY/EXSY homocorrelation displays no exchange crosspeaks, indicating that the Cu atom does not exchange its position between both potentially binding sites of each ligand. In order to detect this type of exchange, we recorded the ^{1}H spectrum of **3b** above the ambient temperature in PhCl-d_5. The first visible effect of warming, detected above 40 ºC, was the broadening of one set of iPr methyls caused by the onset of slow rotation of the non-coordinated N-DiPP group. Heating at higher temperatures had no further effects on the spectrum of **3b** than the expected acceleration of the rotation movement of the

pending aryl group. However, as the temperature was increased the intensity of the spectrum of **3b** decreased in favor of a new set of signals. At 90 ºC the transformation proceeds clean and quantitatively within 2 h. The final spectrum shows signals that were identified as belonging to the free carbodiimide C(=N-DiPP)$_2$ as well as to a new species containing IMe. Analysis of the resulting solution by ESI-MS showed a cluster of signals at m/z 255 with the isotope pattern expected for the cation $[Cu(IMe)_2]^+$ (Scheme 3). The ionic product $[Cu(IMe)_2]^+[BPh_4]^-$, **4**, can be separated from the carbodiimide by washing with diethyl ether the solid residue left after solvent removal, but its crystallization was prevented by its long-term instability in solution, therefore we pursued no further its isolation in crystalline form. A similar compound of composition $[Cu(IMe)_2]^+[OTf]^-$ has been reported in the literature, whose ^{1}H NMR data closely matches those of **4**.[19]

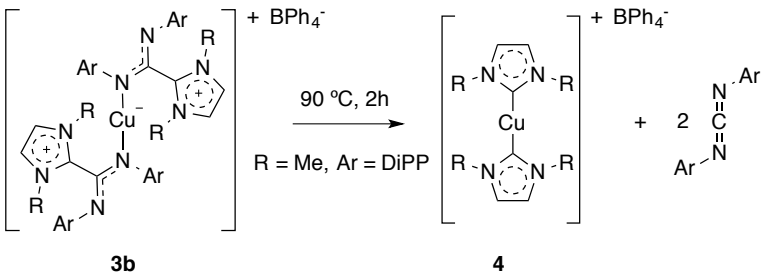

Scheme 3

The reaction shown in Scheme 3 is analogous to the decarboxylation of 2-imidazoliumcarboxylates in the coordination sphere of metals, a facile process that is often used as a mild and effective route to heterocyclic carbene complexes.[8-9] The ready decomposition of **3b** may suggest that similar carbodiimide elimination could also take place from other copper NHC-CDI complexes. Indeed, ^{1}H NMR monitoring of solutions of complexes **1a**, **1b** or **2·BPh$_4$** at 90 ºC provided evidence of the release of the corresponding carbodiimides (CDI^{DiPP} or CDI^{pTol})

and formation of a mixture of unidentified NHC complexes. These processes are significantly slower than the decomposition of **3b**: after 2 h at the mentioned temperature **2·BPh4** decomposes only partially, while the neutral complexes **1a** and **1b** remain essentially unaltered. However, decomposition of the latter was noticeable after longer periods of time. The estimated half-live of **1a** at this temperature is 8.3 h. The decomposition reactions of **2·BPh$_4$** and **1a**,**b** are not completely selective, as ^{1}H NMR monitoring indicates the formation of more than one carbene-containing products.

CONCLUSIONS

Adducts formed by heterocyclic carbenes and carbodiimides (NHC-CDI, or imidazolium-2-amidinates) pose interesting analogies with some key ligands used in catalysis, such as amidinates or α-diimines but, surprisingly, their coordination chemistry has remained hitherto unexplored. We have prepared a series of three such NHC-CDI adducts in a simple, single pot procedure from imidazolium salts and carbodiimides, and prepared several Cu(I) complexes that are the very first examples of their kind.

Depending on the steric hindrance of the NHC-CDI ligands, these can coordinate the Cu(I) center in terminal or bridging mode. Thus, reaction of ICyCDI^{DiPP} or IMeCDI^{DiPP} with copper(I) acetate affords terminally bound complexes of composition **1a** and **1b**, in which the Cu(I) has coordination number 2 and linear geometry. In contrast, the bridging coordination mode becomes more favorable for ICyCDI$^{p\text{-Tol}}$, which gives rise the ionic complex **2·OAc**. In the solid state, this complex contains the trigonal binuclear paddlewheel dication $[Cu_2(ICyCDI^{p\text{-Tol}})_3]^{2+}$, but in solution the acetate ligands and ICyCDI$^{p\text{-Tol}}$ compete for binding the Cu(I) center, giving rise to broad NMR spectra. However, the binuclear paddlewheel structure is

stabilized in solution when acetate ligands are exchanged by the poorly coordinating anion BPh_4^-, which enables informative NMR spectra of the dication to be recorded. Attempts to induce the bulkier IMeCDI^{DiPP} ligand to coordinate in bridging mode by a similar OAc^-/BPh_4^- exchange reaction led to a mononuclear derivative containing two terminally bound ligands, **3b**. In general, Cu(I) NHC-CDI complexes are quite stable in solution at room temperature, but **3b** cleanly eliminates carbodiimide CDI^{DiPP} when heated in solution at 90 ºC, affording the corresponding cationic bis-carbene complex **4**.

EXPERIMENTAL

All operations were carried out under dry nitrogen atmosphere using standard Schlenk techniques. Solvents were rigorously dried and degassed before use. Microanalyses were performed by the Analytical Service of the Instituto de Investigaciones Químicas. NMR spectra were recorded on a Bruker Avance III 400/R spectrometer. ^{1}H and ^{13}C{^{1}H} resonances of the solvent were used as internal standards, but the chemical shifts are reported with respect to TMS. Resonance assignations were routinely aided by using gated ^{13}C, 2D homonuclear H-H COSY and phase-sensitive NOESY, and heteronuclear ^{13}C-^{1}H HSQC and HMBC heterocorrelations. IR and UV-VIS spectra were recorded on Bruker Tensor 27 and Perkin-Elmer Lambda 750 espectrophotometers, respectively. Mass spectra were recorded on a Bruker Esquire 6000 with ESI ion source and ion trap analyzer. *N,N'*-bis(2,6-Diisopropylphenyl)carbodiimide,[20] 1,3-dimethylimidazolium iodide[21] and 1,3-dicyclohexylimazolium tetrafluoborate[22] were obtained according to literature procedures.

Syntheses of ICyCDI^{DiPP}. 4 mL of a 1M solution of a stock solution of KO*t*Bu in THF were diluted to 30 mL in the same solvent. 1.281 g (4 mmol) of *N,N'*-dicyclohexylimidazolium tetrafluoborate ($HICy^+BF_4^-$) were dissolved in 20 mL of THF. The imidazolium salt solution was

magnetically stirred in a cooling bath at -78 ºC, and the KO*t*Bu solution was added drop-wise. Once the addition was finished, the cooling bath was removed, the stirring was continued for *ca*. 30 min, and the mixture was warmed to the room temperature. Then, it was cooled again to -78 ºC and *N,N'*-bis(2,6-diisopropylphenyl)carbodiimide (1.449 g, 4 mmol) dissolved in 10 mL of THF was added drop-wise with stirring. A yellow color developed as the carbodiimide solution was added. The mixture was allowed to warm to room temperature, taken to dryness and the residue extracted several times with 15 mL portions of CH_2Cl_2, until the filtered extracts are very pale or colorless. The combined extracts were evaporated to dryness leaving a yellow solid that was washed with hexane (3 x 10 mL) and dried under vacuum. Yield, 2.140 g., 90 %. X-ray quality crystals were obtained by slow evaporation of a CH_2Cl_2 solution.

^{1}H NMR (400 MHz, CD_2Cl_2, 25 ºC): δ 0.99 (d, 12H, $^3J_{HH}$ = 6.1 Hz, CH*Me*Me); 1.00 (d, 12H, $^3J_{HH}$ = 6.5 Hz, CHMe*Me*); 1.06 – 1.47 (m, 8H, Cy); 1.24 (d, 2H, *J* = 6.9 Hz, Cy); 1.67 (m, 2H, Cy); 1.73 – 1.84 (m, 8H, Cy); 3.13 (h, 4H, $^3J_{HH}$ = 6.8 Hz, C*H*Me$_2$); 4.78 (m, 2H, 1-C*H* Cy); 6.68 (t, 2H, $^3J_{HH}$ = 7.5 Hz, *p*-C*H*$_{arom}$); 6.89 (d, 4H, $^3J_{HH}$= 7.5 Hz, *m*-C*H*$_{arom}$); 7.03 (s, 2H, Imidz). ^{13}C{^{1}H} (100 MHz, CD_2Cl_2, 25 ºC): δ 23.5 (CH*Me*Me); 23.8 (CHMe*Me*); 25.4 (4-*C*H$_2$ Cy); 26.7 (3-*C*H$_2$ Cy); 29.3 (*C*HMe$_2$); 33.8 (2-*C*H$_2$ Cy); 58.6 (1-*C*H Cy); 116.9 (*C*H Imidz); 119.4 (*p*-*C*H$_{arom}$); 122.4 (*m*-C*H*$_{arom}$); 139.7 (*o*-*C*$_{arom}$); 140.2 (*ipso*-*C*$_{arom}$); 146.3 (*C*$_q$ Imidz); 149.1 (*C*(NAr)$_2$). IR (Nujol, cm^{-1}): 3184 (sh, w, ν_{s+as} C-H Imidz); 1593 (m, ν_{as} N=C=N carbodiim); 1541 (br, st, $\nu_{N=C=N}$ δ CH). UV-VIS (CH_2Cl_2): Intense absorption λ_{max} < 200 nm; λ_{max} = 298 nm ($\varepsilon \approx 9.73 \times 10^5$), shoulders at 237 ($\varepsilon \approx 1.12 \times 10^6$), 354 ($\varepsilon \approx 4.37 \times 10^5$) nm. ESI-MS (MeOH) *m/Z* = 595.7 (HM$^+$). Elemental Analysis Calcd. for $C_{40}H_{58}N_4$: C, 80.76; H, 9.83; N, 9.42. Found, C, 80.48; H, 9.68; N, 9.34.

Syntheses of IMeCDI^{DiPP}. A 1 M solution of KO*t*Bu in THF (4 mL, 4 mmol) was added drop-wise to a stirred solution of $HIMe_2^+I^-$ (0.892 g, 4 mmol) in 20 mL of the same solvent, cooled at -78 ºC. Once the addition was complete, the cooling bath was removed and the stirring continued for 10 min, without allowing the mixture to warm to room temperature. Then, the mixture was brought again into the -78 ºC cooling bath and a solution of *N,N'* bis-(2,6-diisopropylphenyl)carbodiimide (1.449 g, 4 mmol) in 15 mL of THF was added with stirring. The mixture was allowed to warm at room temperature, taken to dryness and extracted repeatedly with 10 mL portions of CH_2Cl_2, filtering off the liquid fractions from the solid, until the extracts become colorless. The solvent was evaporated to dryness and the residue was washed with hexane and dried under vacuum, leaving a yellow solid of a paler hue than the ICy betaine derivatives. Yield, 1.744 g, 95 %. X-ray quality crystals were obtained by slow evaporation of a CH_2Cl_2 solution.

^{1}H NMR (400 MHz, CD_2Cl_2, 25 ºC): δ 1.06 (d, 24H, $^3J_{HH}$ = 6.8 Hz, CH*Me*$_2$); 3.38 (h, 4H, $^3J_{HH}$ = 6.8 Hz, C*H*Me$_2$); 3.75 (s, 6H, *N*-Me); 6.78 (t, 2H, $^3J_{HH}$ = 7.5 Hz, *p*-C*H*$_{arom}$); 6.81 (s, 2H, Imidz); 6.95 (d, 4H, *m*-C*H*$_{arom}$). ^{13}C{^{1}H} (100 MHz, CD_2Cl_2, 25 ºC): δ 23.4 (br, CH*Me*Me); 24.5 (br, CHMe*Me*); 28.6 (*C*HMe$_2$); 36.6 (*N*-Me); 120.4 (*p*-*C*H$_{arom}$); 121.2 (*C*H Imidz); 122.6 (*m*-*C*H$_{arom}$); 140.5 (*o*-*C*$_{arom}$); 142.3 (*ipso*-*C*$_{arom}$); 148.7 (*C*(NAr)$_2$); 148.8 (*C*$_q$ Imdz). IR (Nujol, cm^{-1}): 3164 (sh, w, ν$_{s+as}$ C-H Imidz); 1594 (m, ν$_{as}$ N=C=N carbodiim); 1542 (br, st, ν $_{N=C=N}$ and δ CH). UV-VIS (CH_2Cl_2): Intense absorption λ_{max} < 200 nm ; λ_{max} = 254 nm (ε = 1.61 x 10^6), 291 nm (ε = 1.11 x10^6); shoulder at 357 nm (ε = 4.54 x 10^5). ESI-MS (MeOH) *m/Z* = 459.4 (HM$^+$). Elemental Analysis Calcd. for $C_{30}H_{42}N_4$: C, 78.56; H, 9.23; N, 12.21. Found, C, 78.49; H, 9.23; N, 12.21.

Synthesis of ICyCDI$^{p\text{-}Tol}$. 4 mL of a 1M stock solution of KO*t*Bu in THF were diluted to 30 mL in the same solvent. 1.281 g (4 mmol) of *N,N'*-dicyclohexylimidazolium tetrafluoborate

($HICy^+BF_4^-$) were dissolved in 20 mL of THF and the resulting solution was stirred at -78 ºC. The KO*t*Bu solution was added dropwise. Once the addition was finished, the cooling bath was removed and the stirring was continued for *ca*. 30 min while the mixture warmed to the room temperature. The flask was cooled again and *N,N'* bis-di-*p*-tolylcarbodiimide (0.889 g, 4 mmol) dissolved in 10 mL of THF was added dropwise with stirring. A bright yellow color developed as the carbodiimide solution was added. The mixture was allowed to warm to room temperature, taken to dryness and the residue was extracted several times with 15 mL portions of CH_2Cl_2, until the filtered extracts were very pale or colorless. The combined extracts were taken to dryness leaving a bright yellow solid that was washed with hexane (3 x 10 mL) and dried under vacuum. Yield, 1.507 g (83 %). The solid can be recrystallized from a hexane/dichloromethane mixture.

^{1}H NMR (400 MHz, CD_2Cl_2, 25 ºC): δ 1.17 (m, 2H, Cy); 1.40 (m, 8H, Cy); 1.70 (m, 2H, Cy); 1.81 (m, 6H, Cy); 1.86 (br m, 2H, Cy); 2.21 (s, 6H, *p*-Me); 4.57 (m, 2H, 1-C*H* Cy); 6.89 (br s, 8H, *p*-Tol); 6.95 (s, 2H, Imdz). ^{13}C{^{1}H} (100 MHz, CD_2Cl_2, 25 ºC): δ 20.8 (*p*-*C*H_3); 25.4 (4-*C*H_2 Cy); 25.7 (3,3'-*C*H_2 Cy); 33.5 (2,2'-*C*H_2 Cy); 58.5 (*C*H, Cy); 116.4 (CH Imdz); 123.0 (br s, *o*-CH *p*-Tol); 128.7 (*p*-C *p*-Tol); 129.2 (*m*-CH *p*-Tol); 145.1 (*ipso*-C *p*-Tol); 146.8 (C_q Imidz); 150.7 ($C(NAr)_2$). IR (Nujol, cm^{-1}): 3149 (sh, m, ν_{s+as} C-H Imidz); 1609 (m, ν_{as} N=C=N carbodiim); 1530 (br, st, ν N=C=N + δ C-H). UV-VIS (CH_2Cl_2): Intense absorption λ_{max} < 200 nm; shoulders at 230 ($\varepsilon \approx 1.03 \times 10^6$), 308 ($\varepsilon \approx 9.06 \times 10^5$), 358 nm ($\varepsilon \approx 7.96 \times 10^5$). ESI-MS (MeOH) *m/Z* = 455.3 (HM^+). Elemental Analysis Calcd. for $C_{30}H_{38}N_4$: C, 79.25; H, 8.42; N, 12.32. Found, C, 79.66; H, 8.65; N, 12.25.

Syntheses of [Cu(OAc)(ICyCDI^{DiPP})], 1a. A solution of ICyCDI^{DiPP} (0.594 g, 1 mmol) in 15 mL of dichloromethane was added dropwise to a stirred suspension of Cu(I) acetate (0.123 mg, 1

mmol) in the same solvent. The mixture was stirred for 3 h at the room temperature, filtered and the solution taken to dryness. The residue was washed with 20 mL of hexane and dried under vacuum to afford the product as pale yellow solid. Yield, 0.705 g, 98.3 %. X-ray quality crystals were obtained by recrystallization from a dichloromethane/diethylether mixture.

^{1}H NMR (400 MHz, CD_2Cl_2, 25 ºC): δ 0.77 (br s, 12 H, CH*Me*$_2$, free DiPP-*N*); 1.00-1.60 (m, 12H, Cy); 1.29 (d, 6H, $^{3}J_{HH}$ = 6.7 Hz, CH*Me*Me, coord DiPP-*N*); 1.36 (d, 6H, $^{3}J_{HH}$ = 6.7 Hz, CHMe*Me*, coord DiPP-*N*); 1.69 (br s, 3H, OAc, overlapping with Cy signals); 1.71 (d, 2H, $^{2}J_{HH}$ = 12.4 Hz, Cy); 1.79 (d, 2H, $^{2}J_{HH}$ = 12.4 Hz, Cy); 1.92 (d, 2H, $^{2}J_{HH}$ = 12.4 Hz, Cy); 2.71 (h, 2H, $^{3}J_{HH}$ = 6.6 Hz, C*H*Me$_2$, free DiPP-*N*); 2.79 (d, 2H, $^{2}J_{HH}$ = 12.4 Hz, Cy); 3.52 (h, 2H, $^{3}J_{HH}$ = 6.8 Hz, C*H*Me$_2$, coord DiPP-*N*); 4.50 (m, 2H, N-C*H* Cy); 6.74 (t, 1H, $^{3}J_{HH}$ = 7.5 Hz, *p*-C*H*$_{arom}$ coord DiPP-*N*); 6.86 (d, 2H, $^{3}J_{HH}$ = 7.5 Hz, *m*-C*H*$_{arom}$ coord DiPP-*N*); 7.05 (t, 1H, $^{3}J_{HH}$ = 7.1 Hz, *p*-C*H*$_{arom}$ free DiPP-*N*); 7.11 (d, 2H, $^{3}J_{HH}$ = 7.1 Hz, *m*-C*H*$_{arom}$ free DiPP-*N*); 7.18 (s, 2H, C*H* Imidz). ^{13}C{^{1}H} (100 MHz, CD_2Cl_2, 25 ºC): δ 22.3 (br, CH*Me*Me, free DiPP-*N*); 23.4 (CH*Me*Me, coord DiPP-*N*); 23.7 (br , CHMe*Me*, free DiPP-*N*); 25.2 (CHMe*Me*, coord DiPP-*N*); 25.7 (3-*C*H$_2$ Cy); 25.9 (3'-*C*H$_2$ Cy); 26.4 (4-*C*H$_2$ Cy); 29.3 (2 overlapping signals, *C*HMe$_2$); 32.2 (2-*C*H$_2$ Cy); 35.53 (2'-*C*H$_2$ Cy); 59.9 (1-*C*H Cy); 118.7 (*C*H Imidz); 121.8 (*p*-*C*H$_{arom}$, coord DiPP-*N*); 122.9 (*m*-*C*H$_{arom}$ coord DiPP-*N*); 123.4 (*m*-*C*H$_{arom}$ free DiPP-*N*); 124.6 (*p*-*C*H$_{arom}$, free DiPP-*N*); 139.3 (*o*-*C*$_{arom}$ coord DiPP-*N*); 142.3 (*ipso*-*C*$_{arom}$); 143.0 (*C*$_q$); 143.3 (*o*-*C*$_{arom}$ free DiPP-*N*); 143.9 (2 overlapping signals, *C*$_q$). IR (Nujol, cm^{-1}): 3165, 3163 (w, ν$_{s+as}$ C-H Imidz); 1567 (br, ν C=O OAc, ν C=N). UV-VIS (CH_2Cl_2): Intense absorption λ$_{max}$ < 200 nm; shoulders at 270 nm (ε = 3.13 x 10^3), 287 (ε = 2.75 x 10^3) nm. Elemental Analysis Calcd. for $C_{42}H_{61}CuN_4O_2$: C, 70.31; H, 8.57; N, 7.81. Found, C, 70.37; H, 8.85; N, 7.75.

Syntheses of [Cu(OAc)(IMeCDI^{DiPP})], 1b. A Schlenk tube was charged with an equimolar mixture of solid ligand IMeCDI^{DiPP} (0.227 g, 0.5 mmol) and Cu(I) acetate (0.061 g, 0.5 mmol). After adding 20 mL of dichloromethane, the mixture was stirred for 2h at the room temperature, filtered and taken to dryness. The oily residue was stirred with 15 mL of diethylether to afford a pale green solid that was recrystallized from a dichloromethane/toluene mixture to afford the title complex as a pale green crystalline solid. Yield, 74.1 mg, 25 %.

^{1}H NMR (400 MHz, CD_2Cl_2, 25 ºC): Two isomers in 6:1 ratio. *Major isomer*: δ 0.82 (br s, 6 H, CH*Me*Me, free DiPP-*N*); 0.82 (br s, 6 H, CHMe*Me*, free DiPP-*N*); 1.32 (d, 6H, $^3J_{HH}$ = 6.9 Hz, CH*Me*Me, coord DiPP-*N*); 1.37 (d, 6H, $^3J_{HH}$ = 6.8 Hz, CHMe*Me*, coord DiPP-*N*); 1.69 (br s, 3H, OAc); 2.98 (h, 2H, $^3J_{HH}$ = 6.8 Hz, C*H*Me$_2$, free DiPP-*N*); 3.49 (h, 2H, $^3J_{HH}$ = 6.9 Hz, C*H*Me$_2$, coord DiPP-*N*); 3.91 (s, 6H, *N-Me*); 6.79 (t, 1H, $^3J_{HH}$ = 7.5 Hz, *p*-C*H*$_{arom}$ coord DiPP-*N*); 6.87 (d, 2H, $^3J_{HH}$ = 7.5 Hz, *m*-C*H*$_{arom}$ coord DiPP-*N*); 7.02 (s, 2H, C*H* Imidz); 7.08 – 7.18 (m, 3H, C*H*$_{arom}$. freeDiPP-*N*). *Minor isomer*: δ 1.12 (d, 6H, $^3J_{HH}$ = 7.0 Hz, CH*Me*Me); 1.15 (d, 6H, $^3J_{HH}$ = 7.0 Hz, CHMe*Me*); 1.47 (d, 6H, $^3J_{HH}$ = 7.0 Hz, CH*Me*Me); 1.58 (br s, 3H, OAc), 3.18 (h, 2H, $^3J_{HH}$ = 7.0 Hz, C*H*Me$_2$); 3.39 (h, 2H, $^3J_{HH}$ = 7.0 Hz, C*H*Me$_2$); 3.81 (s, 6H, *N-Me*); ^{13}C{^{1}H} (100 MHz, CD_2Cl_2, 25 ºC). *Major isomer*: δ 21.6 (br, CH*Me*Me, free DiPP-*N*); 23.0 (CH*Me*Me, coord DiPP-*N*); 23.9 (br, confirmed in the HSQC spectrum, OAc); 24.8 (br , CHMe*Me*, free DiPP-*N*); 25.7 (CHMe*Me*, coord DiPP-*N*); 28.8 (C*H*Me$_2$, free DiPP-*N*); 29.2, (C*H*Me$_2$, coord DiPP-*N*); 37.0 (*N-Me*); 122.3 (*p*-*C*H$_{arom}$, coord DiPP-*N*); 122.5 (*m*-*C*H$_{arom}$ coord DiPP-*N*); 122.8 (*C*H Imidz); 123.2 (*m*-*C*H$_{arom}$ free DiPP-*N*); 124.8 (*p*-*C*H$_{arom}$, free DiPP-*N*); 139.5 (*o*-*C*$_{arom}$ coord DiPP-*N*); 143.3 (*o*-*C*$_{arom}$ free DiPP-*N*); 143.6 (*ipso*-*C*$_{arom}$ free DiPP-*N*); 144.2, 144.5 (*ipso*-*C*$_{arom}$ coord DiPP-*N* and *C*(N-Ar)$_2$); 145.9 (*C*$_q$ Imidz), 177.6 (Me*C*O$_2$). *Minor isomer*: 21.77 (CH*Me*Me); 24.8 (CHMe*Me);* 28.7 (*C*HMe$_2$), 29.5 (*C*HMe$_2$), 37.1 (*N-Me*); 139.5 (*m*-*C*H$_{arom}$); 142.7 (*m*-*C*H$_{arom}$). IR

(Nujol, cm^{-1}): 3110 (w, ν_{s+as} C-H Imidz); 1596, 1560 (br, ν C=O OAc, ν C=N). UV-VIS (CH_2Cl_2): Featureless spectrum, intense absorption λ_{max} < 200 nm. Elemental Analysis Calcd. for $C_{32}H_{45}CuN_4O_2$: C, 66.12; H, 7.80; N, 9.64. Found: C, 66.48; H, 7.18; N, 9.53.

Synthesis of $[Cu_2(\mu\text{-ICyCDI}^{p\text{-Tol}})_3]^{2+}(OAc^-)_2$, 2-OAc. A solution of the ligand ICyCDI$^{p\text{-Tol}}$ (0.465 g, 0.75 mmol) in 10 mL of dichloromethane was added dropwise to a suspension of Cu(I) acetate (0.228 g, 0.50 mmol) in the same amount of solvent. As the ligand was added, an orange color developed. The mixture was stirred for 2h at room temperature, filtered and taken to dryness. The oily residue was stirred with diethylether to afford a red solid, which was filtered out and dried under vacuum. The solid was recrystallized from CH_2Cl_2/toluene and obtained as red crystals, which were left under vacuum for 24 h in order to remove crystallization solvent. Yield after recrystallization, 0.306 g, 38 %.

^{1}H NMR (400 MHz, CD_2Cl_2, 25 ºC): δ 1.22 (m, 12H, 3-C*H*H Cy); 1.31 – 1.59 (m, 30 H, 2-CH_2 + 4-C*H*H Cy); 1.73 (br d, 6H, $^2J_{HH}$ = 11.4 Hz, 4-CH*H* Cy); 1.87 (br d, 12H, $^3J_{HH}$ = 9.1 Hz, 3-CH*H* Cy); 2.23 (br s, 9H, *p*-Me); 4.39 (br s, 6H, 1-CH, Cy); 6.20 – 7.8 (br m, 24H, CH_{arom}); 7.15 (br s, 6H, C*H* Imidz). ^{13}C{^{1}H} (100 MHz, CD_2Cl_2, 25 ºC): δ 20.8 (*p-Me*); 25.2 (4-*C*H Cy); 25.7 (3-*C*H, Cy); 33.1 (br, 2-*C*H Cy); 34.4 (br, O*Ac*); 59.4 (1-*C*H, Cy); 118.0 (*C*H, Imidz) 120 – 140 (br, *C*H$_{arom}$); 144.4 (br, C_q); 147.5 (br, C_q). IR (cm^{-1}), 1600, 1550 (st, νCO (OAc), ν(CN)). UV-VIS (CH_2Cl_2): Featureless spectrum, intense absorption λ_{max} < 200 nm. ESI-MS (CH_2Cl_2): m/z = 971.5 (Cu(ICyNCN^{ptol})$_2^+$), 744.4 ([Cu_2(ICyCDI$^{p\text{-Tol}}$)$_3$]$^{2+}$). Elemental Analysis Calcd. for $C_{94}H_{120}Cu_2N_{12}O_4$: C, 70.16; H, 7.52; N, 10.45. Found: C, 70.39; H, 7.67; N, 10.59.

Synthesis of $[Cu_2(\mu\text{-ICyCDI}^{p\text{-Tol}})_3]^{2+}(BPh_4^-)_2$, 2-BPh$_4$. $NaBPh_4$ (0.342 g, 0.66 mmol) was dissolved in a mixture of 20 mL of CH_2Cl_2 and 2 mL of THF. Copper(I) acetate (0.123 g, 0.66 mmol) and ICyCDI$^{p\text{-Tol}}$ (0.455 g, 1mmol) were loaded into a Schlenk tube and 20 mL of CH_2Cl_2

were added. The mixture was stirred and the $NaBPh_4$ solution added. The stirring was continued for 2 h at the room temperature, the mixture was filtered and the filtrate was taken to dryness. The red solid residue was extracted with approx. 30 mL CH_2Cl_2, and filtered. Toluene (15 mL) was added and the mixture was stored at -20 ºC overnight to afford a first crop of crystals. The solution was separated, concentrated and cooled again, to yield a second crop. The crystals were collected by filtration, and dried under vaccum. Combined yield, 303 mg, 41 %.

^{1}H NMR (400 MHz, CD_2Cl_2, 25 ºC): δ 0.55 (q, 12H, $^3J_{HH} \approx {}^2J_{HH}$ = 12. 9 Hz, 3-C*H*H Cy); 0.81 (br s, 12H, 2-C*H*H Cy); 1.02 (m, 18H, 2-CH*H* + 4-C*H*H Cy); 1.43 (br d, 6H, $^2J_{HH}$ = 12.9 Hz, 4-CH*H* Cy); 1.53 (br d, 12H, $^3J_{HH}$ = 13.2 Hz, 3-CH*H* Cy); 2.23 (s, 18H, *p*-Me); 3.59 (tt, 6H, $^3J_{HH}$ = 11.8, 2.7 Hz, 1-C*H* Cy); 6.56 (s, 6H, C*H* imidz); 6.61 (d, 12H, $^3J_{HH}$ = 7.8 Hz, *m*-CH_{arom}); 6.85 (t, 8H, $^3J_{HH}$ = 7.1 Hz, *p*-C*H* BPh_4); 6.99 (t, 16H, $^3J_{HH}$ = 7.1 Hz, *m*-C*H* BPh_4); 7.00 (d, 12H, $^3J_{HH}$ = 7.8 Hz, *o*-CH_{arom}); 7.28 (br m, 16H, o-C*H* BPh_4). $^{13}C\{^1H\}$ (100 MHz, CD_2Cl_2, 25 ºC): δ 20.7 (*p*-Me); 25.0 (4-*C*H_2 Cy); 25.3 (3-*C*H_2 Cy); 33.4 (2-*C*H_2 Cy); 59.4 (1-*C*H Cy); 119.7 (*C*H imidz); 122.1 (*m*-*C*H_{arom}); 122.2 (*p*-*C*H BPh_4); 126.0 (m, *m*-*C*H BPh_4); 130.4 (*o*-*C*H_{arom}); 133.0 (*p*-*C*$_{arom}$); 136.3 (*o*-*C*H BPh_4); 140.9 (*C*N_2 Imidz); 142.9 (*C*(N-Ar)$_2$); 146.6 (*ipso*-*C*$_{arom}$); 164.4 (m, *ipso*-*C*, BPh_4). IR (nujol mull, cm^{-1}) 3180 (w, νC-H imidz); 1580 (m, ν C-C ring, BPh_4); 1514, 1461 (br, st, ν NCN), 730, 703 (st, δ C-H arom BPh_4). UV-VIS (CH_2Cl_2): Intense absorption λ_{max} < 200 nm, shoulders at 310 nm, ε ≈ 6000, and 370 nm ε ≈ 3000 mol^{-1} l cm^{-1}. ESI-MS (anisole): m/z = 971.6 ($Cu(ICyNCN^{ptol})_2^+$), 744.4 ($[Cu_2(ICyCDI^{p\text{-}Tol})_3]^{2+}$). Elemental Analysis Calcd. for $C_{138}H_{155}Cu_2N_{12}\cdot CH_2Cl_2$: C, 75.39; H, 7.10; N, 7.59. Found: C, 75.18; H, 6.93; N, 7.19.

Synthesis of $[Cu(IMeCDI^{DiPP})_2]^+[BPh_4^-]$, 3b. A solution of $NaBPh_4$ (0.128 g, 0.38 mmol) in 20 mL of a 9:1 CH_2Cl_2-THF mixture was added to a stirred solution of copper(I) acetate (0.049 g, 0.38 mmol) and ligand $IMeCDI^{DiPP}$ (0.344 g, 0.75 mmol) in 20 mL of CH_2Cl_2. The mixture was

stirred for 2h, then filtered and taken to dryness. The oily residue solidified on stirring with 20 mL of diethyl ether. The solid was filtered out, dried under vacuum and recrystallized from CH_2Cl_2-Et_2O to afford the product as pale yellow microcrystalline material. Yield, 0.352 g, 72 %. X-ray quality crystals were obtained by layering benzene over a concentrate solution of the product in CH_2Cl_2.

^{1}H NMR (400 MHz, CD_2Cl_2, 25 ºC): δ 0.72 (d, 6H, $^3J_{HH}$ = 6.5 Hz, CH*Me*Me, free DiPP-*N*); 0.86 (d , 6H, $^3J_{HH}$ = 7.0 Hz, CHMe*Me*, free DiPP-*N*); 1.08 (d, 6H, $^3J_{HH}$ = 6.8 Hz, CH*Me*Me, coord DiPP-*N*); 1.24 (d, 6H, $^3J_{HH}$ = 6.9 Hz, CHMe*Me*, coord DiPP-*N*); 2.65 (h, 2H, $^3J_{HH}$ = 6.8 Hz, C*H*Me$_2$, free DiPP-*N*); 3.16 (h, 2H, $^3J_{HH}$ = 7.0 Hz, C*H*Me$_2$, coord DiPP-*N*); 3.30 (s, 12H, *N-Me*); 6.35 (s, 4H, C*H* Imidz); 6.81 – 6.91 (m, 6H, C*H*$_{arom}$ free DiPP-*N*); 6,85 (t, 4H, $^3J_{HH}$ = 7.1 Hz, *p*-C*H* BPh_4); 7.02 (t, 8H, $^3J_{HH}$ = 7.4 Hz, *m*-C*H* BPh_4); 7.16 (d, 4H, $^3J_{HH}$ = 6.7 Hz, *m*-C*H*$_{arom}$ coord DiPP-*N*); 7.24 (t, 2H, $^3J_{HH}$ = 6.7 Hz, *p*-C*H*$_{arom}$ coord DiPP-*N*); 7.32 (m, 8H, *o*-C*H* BPh_4). ^{13}C{^{1}H} (100 MHz, CD_2Cl_2, 25 ºC): δ 21.6 (CHMe*Me*, free DiPP-*N*); 23.9 (CH*Me*Me, coord DiPP-*N*); 24.4 (CHMe*Me*, coord DiPP-*N*); 25.0 (CH*Me*Me, free DiPP-*N*); 28.8 (*C*HMe$_2$, free DiPP-*N*); 29.2 (*C*HMe$_2$, coord DiPP-*N*); 36.3 (*N-Me*); 122.2 (*p-C*H BPh_4); 122.9 (*m-C*H$_{arom}$ free DiPP-*N*); 123.0 (*C*H imidz); 123.2 (*p-C*H$_{arom}$ free DiPP-*N*); 124.1 (*m-C*H$_{arom}$ coord DiPP-*N*); 125.3 (*p-C*H$_{arom}$ coord DiPP-*N*); 126.1 (m, *m-C*H BPh_4); 136.3 (*o-C*H, BPh_4); 139.0 (*o-C*$_{arom}$ free DiPP-*N*); 142.8 (*C*$_q$); 143.1 (*C*$_q$); 143.2 (*o-C*$_{arom}$ coord DiPP-*N*); 143.2 (*C*$_q$); 144.2 (*C*N$_2$ Imidz). IR (nujol mull, cm^{-1}): 3125 (w, ν(C-H) imidz); 1553 (m), 1556 (br, st); 1511 (m) (ν(C=N)). UV-VIS (CH_2Cl_2): Featureless spectrum, intense absorption λ_{max} < 200 nm. Elemental Analysis Calcd. for $C_{84}H_{104}BCuN_8$: C, 77.60; H, 8.06; N, 8.62. Found: C, 77.77; H, 7.76; N, 9.00.

Thermal decomposition of 3. A solution of **3** (20 mg, 15 μmol) in C_6D_5Cl (0.6 mL) was heated at 90 ºC for 2h in an air-tight NMR fitted with a J. Young Teflon valve. After this time, the ^{1}H

NMR spectrum showed CDI^{DiPP} and **4.** A sample was taken for ESI-mass spectrometry and the remaining taken to dryness, extracted with Et_2O and filtered. The solution was evaporated again and analyzed by ^1H NMR, which showed the presence of essentially pure CDI^{DiPP}.

Spectroscopic data for **4**: ^1H NMR (400 MHz, C_6D_5Cl, 25 ºC): δ 3.05 (s, 12H, N-*Me*); 6.15 (s, 4H, CH_{imidz}); 6.94 (t, 4H, $^3J_{HH}$ = 7.7 Hz, *p*-C*H* BPh_4); 7.10 (t, 8H, $^3J_{HH}$ = 7.1 Hz, *m*-C*H* BPh_4); 7.80 (br s, 8H,bbb *o-CH* BPh_4). ESI-MS (C_6H_5Cl/C_6D_5Cl): m/z = 255.1 ($[Cu(IMe_2)_2]^+$).

X-ray structure analysis for $ICyCDI^{DiPP}$, $IMeCDI^{DiPP}$, $ICyCDI^{p\text{-}Tol}$, 1a, 1b, 2·OAc, 2·BPh_4 and 3b. Crystallographic data, structure refinement results and fully numbered ORTEP plots for the crystal structures are given in the Supporting Information. Crystals of suitable size for X-ray diffraction analysis were coated with dry perfluoropolyether and mounted on glass fibers and fixed in a cold nitrogen stream (T = 173 K) to the goniometer head. Data collection was performed on a Bruker-Nonius X8Apex-II CCD diffractometer, using monochromatic radiation λ(Mo K_α) = 0.71073 Å, by means of ω and ϕ scans with a width of 0.50 degree. The data were reduced (SAINT)[23] and corrected for absorption effects by the multi-scan method (SADABS).[24] The structures were solved by direct methods (SIR-2002)[25] and refined against all F^2 data by full-matrix least-squares techniques (SHELXTL-6.12)[26] minimizing $w[F_o^2\text{-}F_c^2]^2$. All the non-hydrogen atoms were refined anisotropically, while C-H hydrogen atoms were placed in geometrically calculated positions using a riding model. Some geometric restraints (DFIX command), the ADP restraint SIMU and the rigid bond restraint DELU were used to make the geometric and ADP values of the disordered atoms more reasonable. A search for solvent accessible voids in the crystal structures **2·OAc**, **2·BPh_4** and **3b** using PLATON[27] showed a potential solvent volume, impossible to model even with the most severe restraints. The

corresponding CIF data represent SQUEEZE[28] treated structures, with the undefined solvent excluded from the structural model. The SQUEEZE results were appended to the CIF.

ASSOCIATED CONTENT

Details on the TD-DFT calculation of the UV-VIS spectrum of a model betaine molecule, supplementary crystallographic data and ORTEP views for compounds IMeCDI^{DiPP}, ICyCDI^{pTol}, **2·OAc** and **2·BPh$_4$** (solvent-free crystals) and a list of selected bond lengths and angles for the dication $[Cu_2(\mu\text{-ICyCDI}^{pTol})_3]^{2+}$ in **2·OAc** and both **2·BPh$_4$** structures. This material is available free of charge via the Internet at http://pubs.acs.org.

AUTHOR INFORMATION

Corresponding Author

*Email: campora@iiq.csic.es

ACKNOWLEDGEMENTS

This work was supported by the Government of Spain (Project CTQ2012-30962), Junta de Andalucía (Project FQM6276), and the European Union (FEDER funds). We thank Dr. Gloria Gutiérrez-Alcalá (Mass Spectrometry Service, Instituto de Investigaciones Químicas) for her assistance in the ESI-MS characterization of Cu complexes.

REFERENCES

(1) a) Edelmann, F. T. *Adv. Organomet. Chem.* **2008**, *57*, 183-352. b) Edelmann, F. T. *Adv. Organomet. Chem.* **2013**, *61*, 55-374.

(2) a) Halfpenny, J. C. *Acta Crystallogr. Sect. C: Cryst. Struct. Commun.* **1995**, *51*, 2542-2544. b) Abdou, H. E.; Mohamed, A. A.; Fackler, J. P. *Inorg. Chem.* **2007**, *46*, 9692-9699. c) Berry, J. F.; Bothe, F. A.; Ibragimov, S. A.; Murillo, C. A.; Villagran, D.; Wang, X. *Inorg. Chem.* **2006**, *45*, 4396-4406. d) Jones, C.; Schulten, C.; Rose, R. P.; Stasch, A.; Aldridge, S.; Woodul, W. D.; Murray, K. S.; Moubaraki, B.; Brynda, M.; La Macchia, G.; Gagliardi, L. *Angew. Chem. Int. Ed.* **2009**, *48*, 7406-7410. e) Cotton, F. A.; Daniels, L. M.; Maloney, D. J.; Matonic, J. H.; Murillo, C. A. *Inorg. Chimica Acta* **1997**, *256*, 283-289. f) Chartrand, D.; Hanan, G. S. *Chem. Commun.* **2008**, 727-729. g) Hayawood, J.; Stokes, F. A.; Less, R. J.; McPartlin, M.; Wheatley, A. E. H.; Wright, D. S. *Chem. Commun.* **2011**, *47*, 4120-4122. h) Zall, C. M.; Zherebetskyy, D.; Dzubak, A. L.; Bill, E.; Gagliardi, L.; Lu, C. C. *Inorg. Chem.* **2012**, *51*, 728-736. i) Manowong, M.; Nan, B.; McAlcon, T. R.; Shao, J.; Guzei, I. A.; Ngubane, S.; Van Caemelbecke, E.; Bear, J. L.; Kadish, K. M. *Inorg. Chem.* **2014**, *53*, 7418-7428. j) Tsay, Y. C.; Hsu, C. W.; Shiang, J.; Yu, K.; Lee, G. H.; Wang, Y.; Kuo, T. S. *Angew. Chem. Int. Ed.* **2008**, 7250-7253. k) Dequeant, M. Q.; Bradley, P. M.; Chu, G. L.; Lutterman, D. A.; Turro, C. *Inorg. Chem.* **2004**, *43*, 7887-7892.

(3) a) Ren, T. *Coord. Chem. Rev.* **1998**, *175*, 43-58. b) Pathmore, N. J. *Organomet. Chem.* **2010**, *36*, 77-92.

(4) Collins, S. *Coord. Chem. Rev.* **2011**, *255*, 118-138.

(5) Liu, F. S.; Gao, H. Y.; Song, K. M.; Zhao, Y.; Long, J. M.; Zhang, F. M.; Wu, Q. *Polyhedron* **2009**, *28*, 673-678.

(6) a) Boussie, T.; Murphy, V.; Van Beek, J. A. M. Compositions and Metal Complexes Having Ancillary Ligands, US 6,242,623, June 5, 2011. b) Nelkenbaum, E.; Kapon, M.; Eisen, M. S. *Organometallics* **2005**, *24*, 2645-2659.

(7) Bera, J. K.; Sadhukan, N.; Majumdar, M. *Eur J. Inorg. Chem.* **2009**, 4023-4038.

(8) Delaude, L. *Eur J. Inorg. Chem.* **2009**, 1681-1699.

(9) a) Voutchkova, A. M.; Feliz, M.; Clot, E.; Eisenstein, O.; Crabtree, R. H. *J. Am. Chem. Soc.* **2007**, *129*, 12834-12846. b) Fevre, M.; Pinaoud, J.; Latneur, A.; Gnanou, Y.; Vignolle, J.; Taton, D.; Miqueu, K.; Sotiropoulos, J. M. *J. Am. Chem. Soc.* **2012**, *134*, 6776-6784. c) Delaude, L.; Sauvage, X.; Demonceau, A.; Wouters, J. *Organometallics* **2009**, *28*, 4056-4064.

(10) Kuhn, N.; Steinmann, M.; Weyers, G.; Henkel, G. *Z. Naturforsch. B.* **1999**, *54*, 434-440.

(11) Zhukhovitskiy, A. V.; Geng, J.; Johnson, J. A. *Chem. Eur. J.* **2015**, *21*, 5685-5688.

(12) Martínez-Prieto, L. M.; Urbaneja, C.; Palma, P.; Cámpora, J.; Philippot, K.; Chaudret, B. *Chem. Commun.* **2015**, *51*, 4647-4650.

(13) a) Tanaka, S.; Yagyu, A.; Kikugawa, M.; Ohashi, M.; Yamagata, T.; Mashima, K. *Chem. Eur J.* **2011**, *17*, 3693-3709. b) Cotton, F. A.; Lei, P.; Lin, C.; Murillo, C. A.; Wang, X.; Yu, S. Y.; Zhang, Z. X. *J. Am. Chem. Soc.* **2004**, *126*, 1518-1525. c) Barral, M. C.; Casanova, D.; Herrero, S.; Jiménez-Aaparicio, R.; Torres, M. R.; Urbanos, F. A. *Chem. Eur J.* **2010**, *16*, 6203-6211. d) Cotton, F. A.; Daniels, L. M.; Murillo, C. A.; Schooler, P. *J. Chem. Soc. Dalton Trans.* **2000**, 2001-2005.

(14) Mounts, R. D. O., T.; Fernando, Q. *Inorg. Chem.* **1974**, *13*, 802-805.

(15) a) Woidy, P.; Karttunen, A. J.; Widenmeyer, M.; Niewa, R.; Kraus, F. *Chem. Eur. J.* **2015**, *21*, 3290-3303. b) Hermann, H. L.; Boche, G.; Schwerdtfeger, P. *Chem. Eur. J.* **2001**, *7*, 5333-5342. c) Che, C. M.; Mao, Z.; Miskowski, V. M.; Tse, M. C.; Chan, C. K.; Cheung, K. K.; Phillips, D. L.; Leung, K. H. *Angew. Chem. Int. Ed.* **2000**, *29*, 4084-4088.

(16) Masakawa, M.; Munakata, M.; Kitagawa, S. K. S., T.; Susnaga, V.; Yamamoto, M. *Inorg. Chimica Acta* **1998**, *271*, 129-136.

(17) Straub, B. F.; Rominger, F.; Hofmann, P. *Inorg. Chem.* **2000**, *39*, 2113-2119.

(18) a) Lane, A. C; Vollmer, M. V; Laber, C. H.; Melgarejo, D. Y.; Chiarella, G. M.; Fackler, J. P.; Yang, X; Baker, G. A.; Walensky, J. R. *Inorg. Chem.*, **2014**, *53*, 11357. b) Willcocks, A. M.; Robinson, T. P.; Roche, C.; Pugh, T.; Richards, S. P.; Kingsley, A. J.; Lowe, J. P.; Johnson, A. L. *Inorg. Chem.* **2012**, *51*, 246-257. c) Fan, M.; Yang, Q.; Tong, H.; Yuan, S.; Jia, B.; Guo, D.; Zhou, M.; Liu, D. *RSC Advances* **2012**, *2*, 6599-6605. d) Whitehorne, T. J. J.; Coyle, J. P.; Mahmood, A.; Monillas, W. H.; Yap, G. P. A.; Barry, S. T. *Eur J. Inorg. Chem.* **2011**, 3240-3247. e) Jones, C.; Schulten, C.; Fohlmeister, L.; Stasch, A.; Murray, K. S.; Moubaraki, B.; Kohl, S.; Ertem, M. Z.; Gagliardi, L.; Cramer, C. J. *Chem. Eur J.* **2011**, *17*, 1294-1303. f) Coyle, J. P.; Monillas, W. H.; Yap, G. P. A.; Berry, J. F. *Inorg. Chem.* **2006**, *47*, 683-689.

(19) Raubenheimer, H. G.; Desmet, M.; Lindeque, L. *J. Chem. Resarch (S)* **1995**, 184-185.

(20) Findlater, M.; Hill, N. J.; Cowley, A. H. *Dalton Trans.* **2008**, 4419-4423.

(21) Dinarès, I.; García de Miguel, C.; Ibáñez, A.; Mesquida, N.; Alcalde, E. *Green Chem*. **2009**, *11*, 1507-1510.

(22) Archer, R. H.; Carpenter, J. R.; Hwang, S. J.; Burton, A. W.; Chen, C. Y.; Zones, S. I.; Davis, M. E. *Chem. Mater*. **2010**, *22*, 2563-2572.

(23) APEX2, Bruker AXS Inc.: Madison, Wisconsin, USA, 2007

(24) APEX2, Bruker AXS Inc.: Madison, Wisconsin, USA, 2001

(25) Burla, C. M.; Camalli, M.; Carrozzini, B.; Cascarano, G. L.; Giacovazzo, C.; Poliori, G.; Spagna, R. *J. Appl. Cryst*. **2003**, *36*, 1103.

(26) Sheldrik, G. M. *Acta Crystallogr. A*. **2008**, *64*, 112-122.

(27) Spek, A. L. *Appl. Crystallogr*. **2003**, *36*, 7-13.

(28) v. d. Sluis, P.; Spek, A. L. *Acta Crystallogr. A*. **1990**, *46*, 194-206.

FOR TABLE OF CONTENTS ONLY:

The first complexes containing imidazolium-2-imidinate ligands have been isolated from the reaction of these zwitterionic ligands with copper(I) acetate.